Available online at www.sciencedirect.com
SCIENCE DIRECT
Polymer 47 (2006) 841–848
polymer
www.elsevier.com/locate/polymer

Salt influence upon the structure of aqueous solutions of branched PEO–PPO–PEO copolymers

Christelle Perreur [a], Jean-Pierre Habas [a], Alain Lapp [b], Jean Peyrelasse [a,*]

[a] *Laboratoire de Physico-Chimie des Polymères UMR 5067, Université de Pau et des Pays de l'Adour, Avenue de l'Université, 64000 Pau, France*
[b] *Laboratoire Léon Brillouin, CEA Saclay, 91191 Gif-sur-Yvette, Cedex, France*

Received 19 January 2005; received in revised form 17 November 2005; accepted 23 November 2005
Available online 22 December 2005

Abstract

Triblock copolymers composed of poly(ethylene oxide) (PEO) and poly(propylene oxide) (PPO), present an amphiphilic character in aqueous solution. Since PPO is less hydrophilic than PEO and since their solubilities decrease when the temperature increases, the copolymers self-assemble spontaneously, forming micelles at moderate temperature. For higher temperature or concentration, these solutions can form lyotropic liquid crystalline phases. In order to improve their properties for particular applications, these solutions are often used in the presence of salts. The influence of the salts nature is qualitatively well described for linear copolymer solutions of PEO–PPO–PEO type. The presence of a 'salting out' electrolyte shifts the cloud point and the critical micelle temperature to lower temperature while 'salting in' electrolyte induces opposite effects. In this article, we study the influence of the presence of sodium chloride (NaCl) on the structure of aqueous solutions of a four-branched copolymer. First, we show by viscosimetric studies that NaCl has a 'salting out' effect with these star copolymers as with theirs linear counterparts. Secondly, small angle neutron scattering studies make it possible to determine quantitatively the influence of the NaCl amount on the equilibrium unimers–micelles. These experiments allow obtaining the radius of micelles, their volume fraction and their aggregation number. These informations are compared with the data obtained with salt-free solutions. SANS results are also used to demonstrate that the micelles form bcc polycrystals in a significant zone of the phase diagram. The cell parameter of these crystals is determined according to the salinity of the solution. At last, we observe that the solution presents at high temperature a phase separation. Our results show clearly that this phenomenon is due to the dehydration of the PEO external layer of the micelles.

Keywords: Hydrosoluble copolymer; Salt influence; SANS

1. Introduction

Aqueous solutions of PEO–PPO–PEO blocks copolymers were the topic of numerous studies not only because of their fundamental interest but also of their wide use in many industrial sectors (pharmaceutical, cosmetic, textile, food…). Most of the literature reports deal with linear polymers such as Pluronic® (BASF) or Poloxamers® (ICI). Since PPO is less hydrophilic than PEO, and since their solubility decrease when the temperature increases, the copolymer chains self-assemble spontaneously, forming micelles at moderate temperature. For higher temperature, the polymer or the micelles can form lyotropic liquid crystalline phases that many authors call 'gels'. It is worth to note that these solutions are often used in the presence of additives [1–3,9–12] in order to improve their properties for particular applications such as the manufacturing of electrolytic batteries [4] or drugs delivery [7].

On the basis of literature data, it is clear that the addition of salt in Pluronic aqueous solutions can have two effects that depend on the chemical nature of the salt and/or its concentration. The first one is called 'salting out' effect and is characterized by a decrease in the polymer solubility in water. The presence of a salting out electrolyte shifts the whole gel region, the cloud point and the critical micelle temperature to a lower temperature [7]. Salting out effect is obtained with cations like sodium, potassium, ammonium and anions like sulfate, chloride and bromide. 'Salting in' electrolytes induces opposite effects that are observed with cations like magnesium, aluminium [5] and with anions like ClO_4^-, SCN^-, BF_4^- [13,14]. The salt efficiency seems to vary according to the Hofmeister's series [5–8]. In other words, the 'salting out' effect increases with the multivalency of ions and on the contrary, decreases with growth of the ionic radius.

* Corresponding author. Tel.: +33 5 59 40 77 01; fax: +33 5 59 40 77 44.
E-mail address: jean.peyrelasse@univ-pau.fr (J. Peyrelasse).

0032-3861/$ - see front matter © 2005 Elsevier Ltd. All rights reserved.
doi:10.1016/j.polymer.2005.11.072

Two different mechanisms are proposed to explain the 'salting in' effect [1,2,5]. The first mechanism is described as indirect: salt breaks the 'connections' between polymer and water in order to complex itself with polymer. The complex formed is electrically charged what involves electrostatic repulsion with neighboring units. The second mechanism is known as direct, since in this case, the polymer–solvent bonds are little affected by the salt molecules which are self-associated around the polymer and prevent its dehydration.

On the contrary, the 'salting out' effect is based on a reaction between salt molecules and water that significantly decreases the polymer solubility [5–7].

In the previous study [15], we have characterized the structure and the rheological properties of Tetronic 908® (T908) in aqueous solutions. This compound is a four-branched star copolymer comprised of PEO and PPO blocks fixed on an ethylene diamine. Like its linear counterparts, Tetronic 908 in solution forms micelles under precise conditions of temperature and concentration. In a large zone of the phase diagram the micelles condense according to a body centered cubic lattice (bcc) [16,17]. As a continuation, our present work aims to study the influence of NaCl on the micellization and condensation processes of T908 micelles. Indeed, if it is known that NaCl has a 'salting out' effect, one have only a small number of informations about its influence on the size and structure of micelles and on the nature of the condensed phase. The experimental techniques used in this study are viscosimetry and small angle neutron scattering (SANS).

2. Materials and methods

2.1. Samples

Tetronic® from BASF is a four-branched copolymer. Each branch has the structure $(EO)_x$–$(PO)_y$ where EO and PO define, respectively, ethylene oxide and propylene oxide. The four branches are linked by a PO unit to an ethylene diamine. The polymer studied in this study, is commercially known as T908. The numbers of EO and PO units per branch are, respectively, $x=114$ and $y=21$. Thus, its molecular weight is $M_w=25{,}000\ g\ mol^{-1}$. This copolymer was used as received without further purification. Solutions were prepared by mixing the copolymer with water at low temperature. Bi-distilled water was used for all rheological experiments while deuterated water, D_2O, was used for the small angle neutron scattering studies. In the framework of our study, the weight percentage p of polymer in solutions is kept constant and equal to 30 wt%. NaCl was purchased from the Prolabo Society, its molarity is expressed in M units so that $a\,x\,M$ solution defines a solution containing $x\ mol\ L^{-1}$ of salt.

2.2. Experimental techniques

Measurements of the kinematic viscosity η_k were performed using Ubbelohde glass capillary tubes commercialized by the Schott–Geräte Society. The collection of the data is automatically performed by a viscotimer S1 from Lauda Company. SANS experiments were realized at the laboratoire Léon Brillouin, CEA de Saclay (France) on the PAXY spectrometer. The neutron wavelength selected was $\lambda=6$ Å (with a resolution of 10%) and the effective distance between the sample and the detector was 3.1 m. Quartz cells were used with 2 or 1 mm path length for static measurements. References and data corrections have already been specified elsewhere [15]. In order to perform measurements under shear, we used a thermostated Couette cell made of quartz. The external cylinder was mobile ($\Phi=47.24$ mm) around a vertical axis, while the internal cylinder ($\Phi=43.43$ mm) was fixed. The height of the inner cylinder was 55 mm. The cell was positioned so that the neutron beam was perpendicular to the rotation axis. According to the geometry, the shear-rate range was comprised between 0 and 955 s^{-1}.

3. Results

3.1. Viscosity and phase diagram

On Fig. 1, are represented according to the temperature, the variations of the kinematic viscosity of a 30 wt% solution of T908 in the presence of 0.05 M of NaCl. In the low temperature range, up to the temperature T_1, the plot $\ln(\eta_k)=f(1/T)$ is a straight line. This shows that the viscosity of the solution varies according to Arrhenius law as currently observed with classical liquids. By comparison of the viscosimetric results with the data got by other experimental techniques (light scattering, small angle neutron scattering), we showed [15] for solutions in pure water that T_1 corresponds to the critical temperature of micellization (CMT).

Beyond T_1, the increase in viscosity could be due to the displacement of the equilibrium unimers–micelles in favor of micelles that involves an increase in their volume fraction. This interpretation will be validated by SANS results. At the temperature T_2, the viscosity diverges: the solution does not flow any more and looks like a gel. The structure of condensed phase for $T>T_2$ will also be determined by SANS on samples in steady flow.

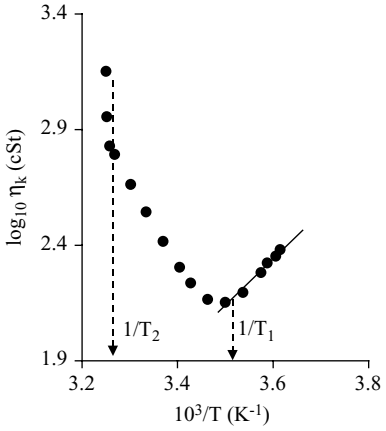

Fig. 1. Evolution of the logarithm of the kinematic viscosity of a 30 wt% solution (0.05 M of NaCl) as a function of the reciprocal of the absolute temperature.

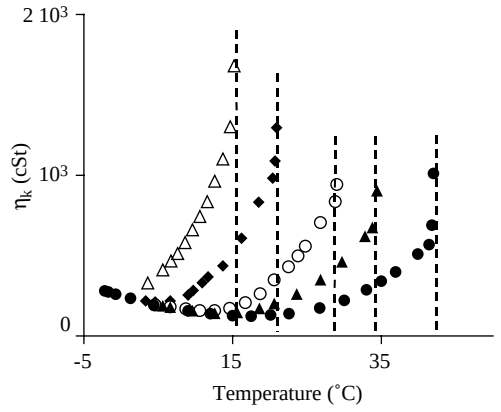

Fig. 2. Effect of temperature on the viscosity of 30 wt% T908 solutions with different amounts of NaCl: 0 M (●), 0.05 M (▲), 0.1 M (○), 0.5 M (◆), 1 M (△). The broken lines indicate the temperatures of the viscosity divergence.

Fig. 2 presents the evolution of the kinematic viscosity according to temperature for T908 in aqueous solutions containing different amounts of sodium chloride.

It can be noted that when the concentration of NaCl increases, the temperature T_2 of the viscosity divergence is shifted to lower values. Moreover, the most salted solutions present at the temperature T_3 a phase separation with clouding that has not been observed until 95 °C for solutions in pure water. In the Fig. 3, we have reported the temperatures T_1, T_2 and T_3 in order to define the phase diagram of 30 wt% aqueous solutions of T908 according to the amount of dissolved salt.

One can note that the zone where the solution only contains unimers is very small. It is also showed that the solutions of salinity higher than 2.5 M are in a condensed state even at the lowest accessible temperatures. Moreover, the cloud point temperature decreases very quickly with the salt concentration. These results demonstrate that the sodium chloride strongly decreases the polymer solubility in water. This result agrees with the conclusions of previous studies on linear triblocks copolymers of PEO–PPO–PEO type [7,18–20].

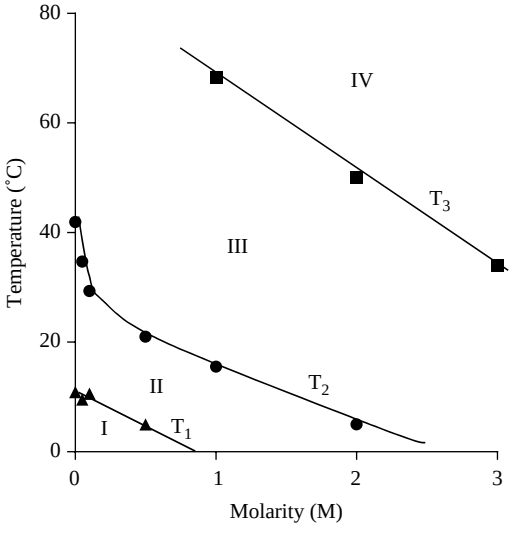

Fig. 3. Influence of NaCl content upon the phase diagram of a 30 wt% solution of T908. I, unimers; II, unimers + micelles; III, condensed phase; IV, two phases.

3.2. Small angle neutron scattering studies

We have completed these viscosimetric measurements with SANS experiments to obtain quantitative informations about the effects of NaCl on the structure of the solutions. We carried out measurements on aqueous solutions of T908 ($p = 30$ wt%) for different salt concentrations (0.05, 1 and 3 M).

In a neutron scattering experiment, one measures the diffused intensity I according to the wave vector modulus $q = (4\pi/\lambda)\sin(\theta/2)$ (where θ is the scattering angle). Fig. 4 represents the evolution of the diffused intensity according to temperature for a 30 wt% solution with 0.05 M of NaCl. In the zone I of the phase diagram, the diffused intensity remains weak and is not dependent on q (Fig. 4, $T = 5$ °C). This result is the characteristic of a homogenous mixture. It assesses that the polymer is not micellized in this zone of the phase diagram.

In zone II of the phase diagram, the $I(q)$ curves present a peak that is the characteristic of the micelles presence. It is worth to note that its intensity increases with temperature (Fig. 4, $T = 10$, 16 and 34 °C).

In the zone III of the phase diagram, two small secondary peaks appear on the $I(q)$ curves (Fig. 4, $T = 54$ °C). If q_1, q_2 and q_3 designate the positions of the successive peaks, the ratios q_2/q_1 and q_3/q_1 are about equal to $\sqrt{2}$ and $\sqrt{3}$. This means that the micelles are ordered according to a simple or body centered cubic lattice.

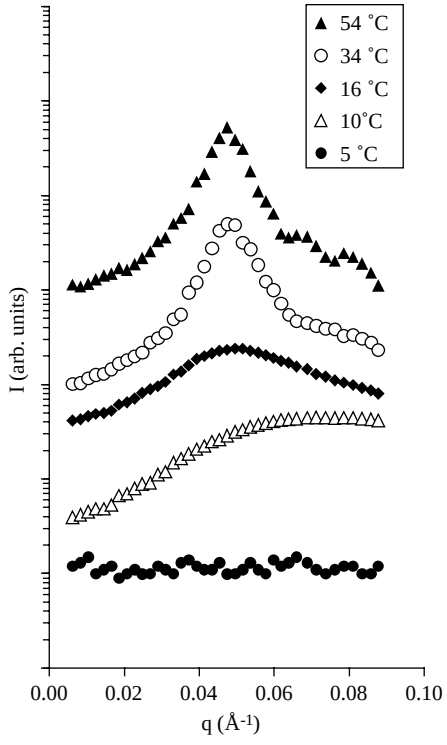

Fig. 4. Scattered intensity of a 30 wt% solution with 0.05 M NaCl at different temperatures. For clarity, the curves have been arbitrarily shifted along the y-axis.

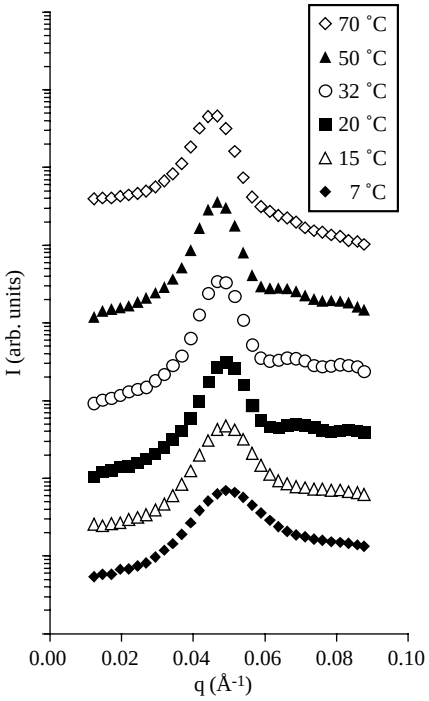

Fig. 5. Scattered intensity of a 30 wt% solution with 1 M NaCl at different temperatures. For clarity, the curves have been arbitrarily shifted along the *y*-axis.

On Figs. 5 and 6, are reported the results, obtained with the 1 and 3 M solutions. Even at the lowest temperature, one observes a peak on the $I(q)$ curves. This confirms that the critical temperature of micellization is strongly lowered when the salinity increases. These experiments also show that

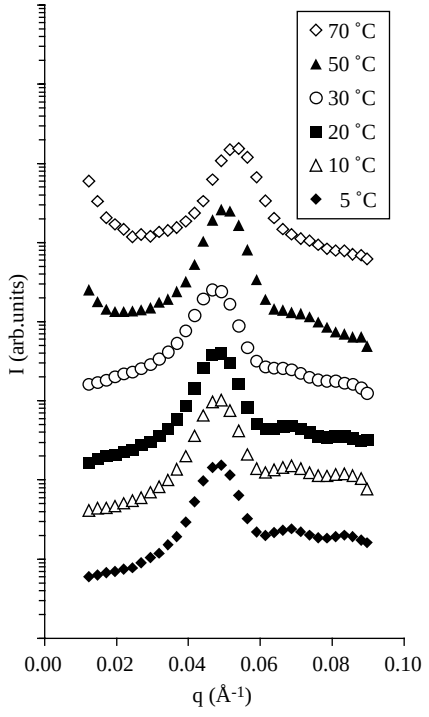

Fig. 6. Scattered intensity of a 30 wt% solution with 3 M NaCl at different temperatures. For clarity, the curves have been arbitrarily shifted along the *y*-axis.

the higher order peaks appear at lower temperatures. The beginning of the condensation process is detected at 5 and 20 °C for the solutions containing, respectively, 3 and 1 M of salt while it begins at 42.6 °C for the salt free solution. All these results are perfectly coherent with the limits of the phase diagram determined by the viscosimetric study.

Moreover, for the 3 M solution, one can note on the Fig. 6 and for $T \geq 50$ °C, an increase in $I(q)$ at low q. This phenomenon is a consequence of the formation of large aggregates in the vicinity of the phase separation temperature. In the same time, the intensity of the main peak decreases and the secondary peaks disappear revealing that the liquid crystal organization is destroyed in this temperature range. This phenomenon is particularly clear with the 3 M solution at 70 °C.

4. Structure of the micelles

To explain the results obtained for T908 solutions in pure water, we have developed in the previous paper [15] a model that provides several structural informations.

The theoretical expression of the scattered intensity is given by the relation:

$$I(q) = N\Delta\rho^2 P(q)S(q)$$

where N is the number of micelles by unit volume, $\Delta\rho^2$ is the contrast factor, $P(q)$ is the form factor, and $S(q)$ the structure factor.

The expression of $S(q)$ depends on the interaction potential between micelles. For diluted solutions, for which the micellar correlation are negligible, $S(q) = 1$. The form factor depends on the model chosen to describe the micelles. The simplest model is that of Mortensen et al., who assume a monodisperse suspension of dense spheres with a sharp interface [21,22]. Mortensen et al. have postulated that the core of radius R_c, contains all the PPO and a small percentage of PEO which is not possible to detect since the scattering length density of EO and PO are close. The major part of PEO forms a hydrated corona, but the authors neglected its presence in their calculations. Then, the form factor $P(q)$ is that of a hard sphere of radius R_c. In their model, the various adjustable parameters are the equivalent hard sphere radius R_{hs}, the volume fraction of hard sphere ϕ_{hs} and the core radius R_c. This model does not allow calculation of the aggregation number (number of unimers per micelles), but the most important was the omission of the corona whose contrast cannot be considered equal to that of water, above all when the latter contains the majority of PEO units.

Goldmints et al. used a two shells model where the micelle was assimilated to a core of radius R_c surrounded by a corona of radius R_m [23,24]. The authors set different hypotheses: the radius R_m of the micelle was assumed identical to the radius of the hard sphere $R_m = R_{hs}$, the scattering length densities of PO and EO are equal, water is present both in the core and the corona of the micelle.

Liu et al. [25] also used a two-shells model in which the core of the micelle was made of PO units under close packing conditions and the corona was considered as an homogenous mixture of PEO and water. They assume that all the polymer was micellized. In addition to take into account the possible attractive interactions occurring between micelles, they assume that hard spheres are adhesive. This model required the introduction of two additional parameters in the structure factor: the surface adhesion potential and the fractional surface layer thickness.

The two previous models present some problems. Goldmints's and Liu's models require the knowledge of the aggregation number, which can only be determined if we know the equilibrium between unimers and micelles at each temperature and concentration. Goldmints supposes that at a fixed temperature, the fraction of unimers is independent of the initial concentration of the solution and is equal to the CMC. If this hypothesis may be correct for low concentrated solutions, it may not be relevant for the polymer solutions of high volume fraction that we have studied.

In the preceding paper [15], we have tried to fit the neutron scattering curves of Tetronic 908 solutions in pure water with the different models previously outlined. We showed that Mortensen's and Goldmints's models correctly describe the position and the amplitude of the peak. As these parameters are governed by the structure factor, we can think that these models give good estimates of the volume fraction and radius of the micelles. Both models considerably deviate, however, from experimental data at low and high values of q. This shows that the micellar structure is not well described. As regards Liu's model, the peak is overestimated which is due to not taking into account the important fraction of unmicellized polymer.

We tried to improve the two layers model. We assume hard sphere interactions between micelles. The first layer that is the core of the micelle, contains all the PO units in compact packing. The second layer contains hydrated PEO. We assume also that there is an equilibrium between unimers and micelles and we introduce as additional parameter the fraction of micellized polymer F_p (F_p is the ratio of the mass of micellized polymer to the total mass of polymer in the solution). The three parameters are the radius of the micelle, the volume fraction of micelles (or aggregation number) and the fraction of micellized polymer. It is obvious on Fig. 7 that this model does not explain correctly the results obtained. Introduction of water into the core of the micelle does not improve the results.

Then, we established a three-layers model. The fundamental hypothesis is that all micelles are identical, spherical and coexist in equilibrium with unimers at each temperature. The first layer that is the core of the micelle is made up of all the PO units in compact packing. The second one is a dense layer of PEO and the last one is formed by strongly hydrated PEO. This model uses four parameters: the volume fraction ϕ and the radius R_m of micelles, the fraction of PEO in the dense layer and the fraction of micellized polymer F_p. Then, it is possible to determine the radius of the core, the aggregation number N_{agg} and the hydration rate of the micellar corona ϕ_W which is

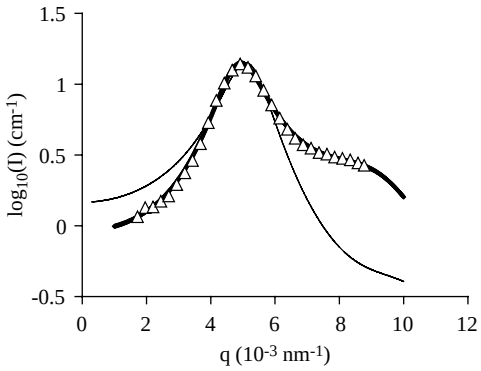

Fig. 7. Scattered intensity of a 30 wt% solution with 1 M NaCl at 7 °C. Symbols: experimental points. The thin line is a fit with a two-shell model. The bold line is a fit with our three-shell model.

the ratio of the volume of water in the corona upon their total volume. This model was initially developed for salt-free solutions and the details of the mathematical development can be found in Ref. [15]. As one can see it on the Fig. 7 this model is also powerful enough to describe the experimental $I(q)$ curves of solutions with salt. In the example of Fig. 7, the mean percentage error is very small for the three-shell model (3%) but it reaches 40% for the two-shell model.

The model allows also the fitting of the $I(q)$ curves in the cubic zone because the secondary peaks have a very low intensity. it is for that, that the values of the parameters obtained by the iteration process are not affected by a cutback of the $I(q)$ curve that excludes the secondary peaks.

All structural parameters obtained from the model for salted solutions are compared to values get for the salt-free system. The evolution of the fraction of micellized polymer according to temperature is presented on the Fig. 8 for four solutions (0, 0.05, 1 and 3 M). For salt-free solutions or containing a small amount of NaCl (0.05 M), the extrapolation of the curve to $F_p = 0$ makes it possible to define the critical temperature of micellization that is in good agreement with the phase diagram previously determined (Fig. 3). We can also notice that F_p quickly increases with the temperature just above the CMT. This shows that the equilibrium unimers–micelles is shifted in favor of micelles when the temperature increases but this

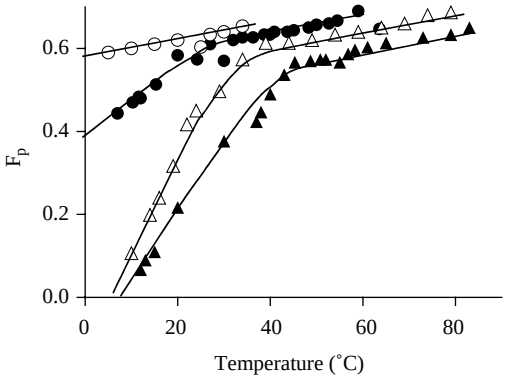

Fig. 8. Evolution of the fraction of micellized polymer (T908—30 wt%) versus temperature for different amounts of NaCl: 0 M (▲), 0.05 M (△), 1 M (●), 3 M (○). The solid lines are guides for the eyes.

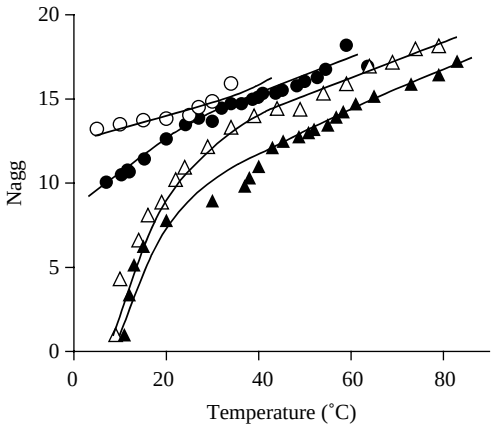

Fig. 9. Evolution of the aggregation number (T908—30 wt%) versus temperature for different amounts of NaCl: 0 M (▲), 0.05 M (△), 1 M (●), 3 M (○). The solid lines are guides for the eyes.

increase is more rapid for salted solutions (0.05 M) than for the salt-free solution.

For 1 M solution, the fraction of micellized polymer is significant even at lowest temperatures. This shows that the 'unimer' zone is out of the experimental range for these salt concentrations. This result is still in agreement with the phase diagram obtained from viscosity measurements.

In the zone where the micelles are ordered, (that is to say in the whole temperature range for the 3 M solution), in spite of the very great viscosity of the medium, the diffusion of the unimers is still possible, since F_p continues to increase with the temperature. In addition at high temperatures, one can notice that the larger the salinity, the higher F_p is.

Fig. 9 represents the variations of the aggregation number as a function of temperature. One can note that the curves obtained with the different salinities, present shapes that resemble the ones representing the F_p variations. This seems to indicate that the unimers passing in a micellar state will enlarge preferentially existing micelles rather than to form new micelles.

It is also interesting to observe that the values of the aggregation numbers are much smaller than the ones that are announced in the literature for solutions of $(EO)_x$–$(PO)_y$–$(EO)_x$ linear copolymers. Indeed, as regards Pluronic F127 solutions ($x=99$, $y=65$), Mortensen [27] obtains $N_{agg}=58$ at 20 °C and 116 at 40 °C. Liu et al. [21] for P84 solutions ($x=19$, $y=43$) propose similar values although the polymers used have very different chains lengths. In our case, the maximum value obtained is $N_{agg}=18$ showing that the aggregation process is obstructed by the branched structure of the T908.

Fig. 10 represents the evolution of the volume fraction of micelles according to the temperature. For all salinities studied, it is not surprising to show that ϕ evolves in a similar way as F_p in the low temperature region. However, it is to note that in the zone where the micelles are ordered, the volume fraction becomes constant (close to 0.49) and not dependent on the quantity of salt dissolved in the solution. This critical volume fraction corresponds to the theoretical value for the crystallization of hard spheres [26].

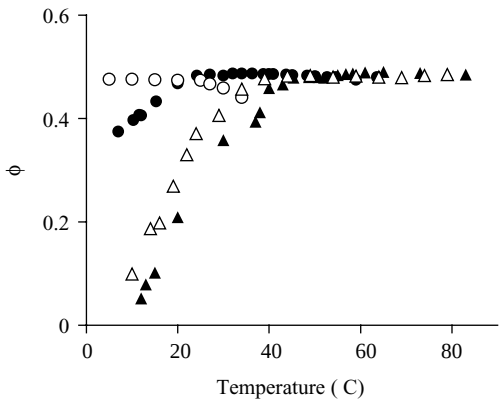

Fig. 10. Evolution of the volume fraction of micelles (T908—30 wt%) versus temperature for different amounts of NaCl: 0 M (▲), 0.05 M (△), 1 M (●), 3 M (○).

Fig. 11 shows the evolution of the radius of micelles according to the temperature. Excepted for the most salted solutions, the radius of micelles quickly increases above the critical temperature of micellization as F_p or N_{agg}. Then, it varies slightly in the zone where the micelles are ordered. This is clear for the 3 M solution where R_m remains practically constant in the temperature range studied.

Our model also allowed the determination of the evolution of the hydration rate of the micellar corona according to the temperature (Fig. 12). In the case of solution in pure water, after an initial rapid decrease at low temperature, the hydration rate of the corona varies little in the temperature range studied. Fig. 12 shows also that the hydration rate decreases when the salt concentration increases at a fixed temperature. This observation is useful to understand why the micelles radii are quasi independent on the salinity of the solution at high temperature whereas the aggregation number increases with the salt content. In other words, at a given temperature, the increase in the radius due to the augmentation of the aggregation number is counterbalanced by a reduction of the hydration of the micellar corona.

It is interesting to examine more particularly the results obtained with the 1 and 3 M solutions. Indeed, in the vicinity of

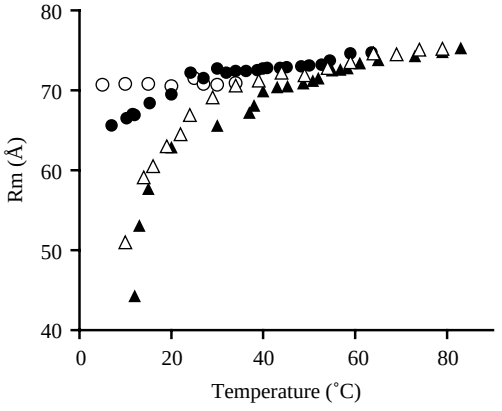

Fig. 11. Evolution of the radius of micelles (T908—30 wt%) versus temperature for different amounts of NaCl: 0 M (▲), 0.05 M (△), 1 M (●), 3 M (○).

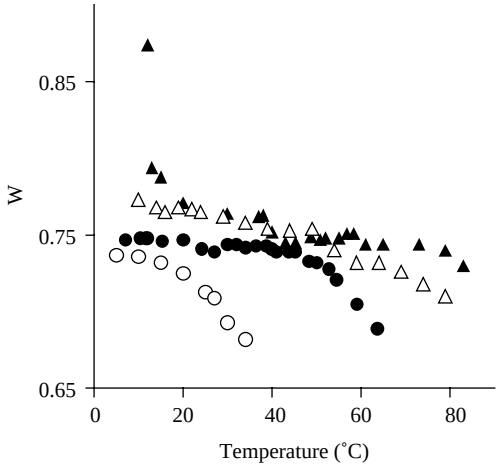

Fig. 12. Evolution of the hydration rate of the external shell (T908—30 wt%) versus temperature for different amount of NaCl: 0 M (▲), 0.05 M (△), 1 M (●), 3 M (○).

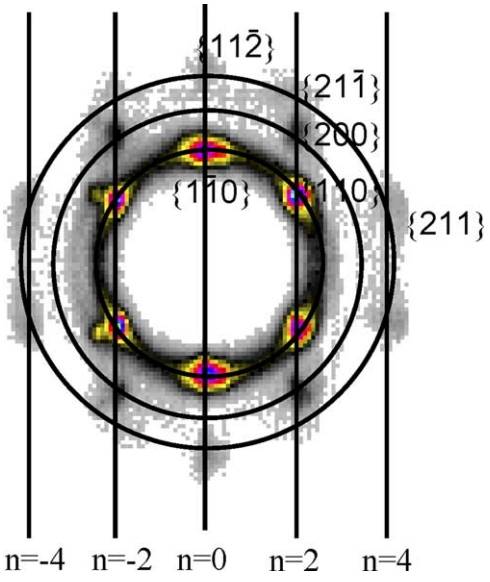

Fig. 13. Diffraction pattern under shear of a 30 wt% solution with 1 M NaCl.

the cloud point, it is worth to note a very fast dehydration of the micelles. This demonstrates that the solubility reduction of PEO units in water is at the origin of the phase separation phenomenon. This result also agrees with the conclusions of Jain et al. [19], obtained with Pluronic P84 and P104 solutions containing a small quantity of KCl. Indeed, they show that the number of water molecules that are attached to each ethylene oxide unit in the hydrated PEO shell, decreases with increasing salt concentration. As expected, the addition of NaCl to Tetronic solution has a salting out effect.

5. Long range structure

We have demonstrated in Section 3 of this paper, that in a broad zone of the phase diagram, the micelles are ordered according to a cubic lattice. When the solution is not sheared, the 2D diffusion patterns are isotropic. This shows that the polycrystals have all possible orientations in space. Under flow, the diffraction pattern becomes anisotropic as shown in Fig. 13.

The diffraction spots are distributed in vertical and equidistant layers, as well as in concentric circles. The spots that are located on the same circle have the same scattering angle. According to the Bragg's relation ($2d_{hkl}\sin(\theta/2)=\lambda$), this is the characteristic of diffraction through reticular planes with the same d_{hkl}. The diffraction pattern looks like X-ray diffraction diagram obtained by the crystal rotation method. In this latter, a mono-crystal is rotated around an $[u,v,w]$ row. During the rotation, each reticular plan having an angle to the incident beam that satisfies the Bragg relation makes possible a reflection. The result is a spot diagram like the one observed on Fig. 13. The spots of the layer of order n are due to the diffraction by the reticular planes $\{h,k,l\}$ that verify the equation:

$$uh + vk + wl = n$$

The distance between the layers is given by:

$$\Delta = \frac{D\lambda}{L}$$

where D is the distance between the sample and the detector and λ the wavelength. L is the distance between two consecutive nodes on the $[u,v,w]$ row.

To explain our results, we assume that the scattering pattern is due to an ensemble of different crystalline domains of all orientations, but with a direction $[u,v,w]$ aligned along the flow. From an experimental point of view, the results obtained will be identical to the ones using a mono-crystal rotating around the same direction.

The only way to explain the scattering pattern is then to assume a body centered cubic lattice for which crystals orient themselves with the [1,1,1] direction in the direction of the flow. In this case, the spots of layer n satisfy: $h+k+l=n$ and all the spots predicted by theory, can be observed and indexed until the third order as shown in Fig. 13.

Knowing now that the micelles are ordered according to a bcc lattice, it is possible to calculate the cell parameter a from the position q_1 of the main peak. For the bcc cubic lattice, the main peak is due to the diffraction by {0,1,1} reticular planes characterized by $d_{110}=a/\sqrt{2}$. With the definition of q and the Bragg relation this leads to $a=2\pi\sqrt{2}/q_1$. We have calculated a for different solutions in a large temperature range (Fig. 14). Except for the 3 M solution, the cell parameter varies linearly with the temperature, the dilatation coefficient is close to $4\times 10^{-3}\,°C^{-1}$. In addition, even if one notes a small increase with the content salt, there are no fundamental differences with the cell parameter obtained with salt free solutions [16,17]. For the 3 M solution, the determination of the lattice parameter is much more difficult since the organization is destroyed very quickly in the vicinity of the phase separation temperature, but

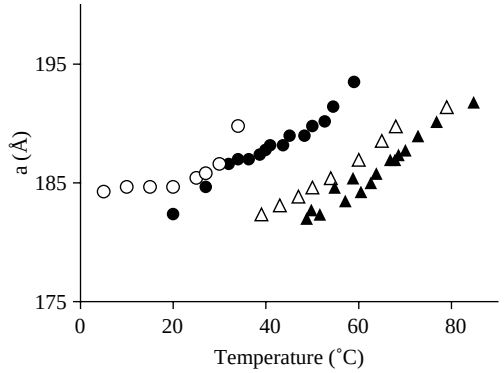

Fig. 14. Evolution of the cell parameter of the bcc network as a function of temperature. 0 M (▲), 0.05 M (△), 1 M (●), 3 M (○).

the a values are very close to the one calculated for the 2 M solution at the same temperature.

6. Conclusion

Our article shows that NaCl addition in aqueous solution of branched PEO–PPO–PEO copolymers produces a 'salting out' effect as for solutions of linear copolymers: the different transition temperatures (micellization, condensation, phase separation) are shifted to lower temperatures. The model initially developed for pure solution, is able to describe also the SANS scattered intensity of solutions in presence of salt. It shows that above the critical micelle temperature the micelles are in equilibrium with unimers. It also allows the determination of the structure of the micelles. The aggregation number, the radius of the micelles and the water content of the outer corona were determined as a function of temperature and salt content. When the temperature increases, the fraction of micellized polymer increases what involves the growth of the aggregation number. In the temperature range where the micelles are ordered, the fraction of micellized polymer and the aggregation number are slightly higher than the ones obtained with salt-free solutions. However, if the hydration rate of the corona is smaller in presence of salt, the radius of the micelles and their volume fraction are about the same, independently of the salt amount.

SANS measurements performed on samples under flow reveal that the condensed phase remains bcc as for salt-free solutions. If the cell parameter slightly increases with the salt content there are no fundamental differences with solutions in pure water.

References

[1] Cardoso Da Silva R, Loh W. Colloid Interface Sci 1998;202:385.
[2] Alexandridis P, Athanassiou V, Hatton AT. Langmuir 1995;11:2442.
[3] Mansur CRE, Spinelli LS, Oliveira CMF, Gonzalez G, Lucas EF. J Appl Polym Sci 1998;69:2459.
[4] Bakker A, Lindgren J, Hermansson K. Polymer 1996;37:1871.
[5] Pandya K, Lad K, Bahadur P. Pure Appl Chem 1993;A30:1.
[6] Bahadur P, Pandya K, Almgrem M, Li P, Stilbs P. Colloid Polym Sci 1993;271:657.
[7] Pandit N, Trygstad T, Croy S, Bohorquez M, Koch CJ. Colloid Interface Sci 2000;222:213.
[8] Carale TR, Pham QT, Blankstein D. Langmuir 1994;10:109.
[9] Wu G, Chu B. Macromolecules 1994;27:1766.
[10] Wu G, Chu B, Ying Q. Macromolecules 1994;27:5758.
[11] Zhou S, Su BCJ. J Polym Sci 1998;36(Part B):889.
[12] Homqvist P, Alexandridis P, Lindman B. Macromolecules 1997;30:6788.
[13] Schott H. J Colloid Interface Sci 1997;189:117.
[14] Jorgensen EB, Hvidt S, Brown W, Schullen K. Macromolecules 1997;30:2355.
[15] Perreur C, Habas J-P, Peyrelasse J, François J, Lapp A. Phys Rev E 2001;63:31505.
[16] Perreur C, Habas J-P, Francois J, Peyrelasse J, Lapp A. Phys Rev E 2002;65:41802.
[17] Habas J-P, Pavie E, Perreur C, Lapp A, Peyrelasse J. Phys Rev E 2004;70:61802.
[18] Jain NJ, George A, Bahadur P. Colloids Surf 1999;157:275.
[19] Jain NJ, Aswal VK, Goyal PS, Bahadur P. Colloids Surf 2000;173:85.
[20] Lenaerts V, Triqueneaux C, Quarton M, Rieg-Falson F, Couvreur P. Int J Pharm 1987;39:121.
[21] Mortensen K, Pedersen JS. Macromolecules 1993;26:805.
[22] Mortensen K, Brown W, Jorgensen E. Macromolecules 1994;27:5654.
[23] Goldminst L, von Gottberg FK, Smith KA, Hatton TA. Langmuir 1997;13:3659.
[24] Goldminst L, Yu GY, Booth C, Smith KA, Hatton TA. Langmuir 1999;15:1651.
[25] Liu YC, Chen SH, Huang JS. Phys Rev E 1996;54:1698.
[26] Hoover WG, Ree FH. J Chem Phys 1968;49:3609.
[27] Mortensen K. J Phys: Condens Matter 1996;8:103.